Optical Fiber Phase Noise Cancellation for Slow Light Crystal Cavity Locking

Mohammad Tasnimul Haque
Supervisor: Lars Rippe

Master Thesis
May 2016

LUND UNIVERSITY

Department of Physics
Atomic Physics Division

Abstract

Recent developments in the field of optical clocks and quantum information have fueled the necessity for both fiber phase noise cancellation and laser stabilisation. The Quantum Information group at Lund University is conducting research on quantum computation experiments based on rare earth ion doped crystals and also application of slow light effects induced by spectral hole burning in these rare earth ion doped crystals. Slow light effects can significantly improve laser stabilisation by increasing effective cavity length without inducing mechanical noise. In this thesis a fiber phase noise cancellation setup was designed and built. The fiber stabilisation will be used in a setup where a laser is stabilised using a slow light crystal cavity as frequency reference and a setup was designed for this application.

By partially reflecting back light through a fiber and by performing a phase measurement and through feedback control, the fiber phase noise can be effectively cancelled. A method for first creating a slow light crystal cavity and then locking the laser to one of the resonance peaks of the cavity was planned and designed incorporating two fiber locking setups for phase noise cancellation. Suitable components for building the system was investigated and put together. Fiber locking experiment was then carried out.

Acknowledgement

This thesis project was done at the Atomic Physics division of Lund University as a partial requirement for fulfillment of my master education in Photonics and would not have been possible without the kindly help of several persons. First of all, I would like to thank my supervisor Lars Rippe who has always encouraged me to think through the step by step planning and design process for the project, was always willing to answer questions with a kindly smile and also for helping and guiding me in the lab whenever possible. Secondly, I would like to thank Stefan Kroll for providing me the opportunity to do the master project in the quantum information group and for always being concerned and insightful. I would also like to thank the other group members, Qian and Adam for their warm friendly welcome and support in the lab. The drawings in the thesis was done using software Inkscape and I would like to acknowledge Alexander Franzen for developing the component library. I would also like to thank Swedish Institute for providing me a scholarship which covered the costs of my master education for last two years. Finally, I would like to thank my family members and friends for always inspiring me to do research work.

List of Figures

List of Abbreviations

AC	Alternating Current
AOM	Acousto -Optic Modulator
DC	Direct Current
DDS	Direct Digital Synthesizer
EOM	Electro- Optic Modulator
GPS	Global Positioning System
LFGL	Low Frequency Gain Limit
PDH	Pound - Drever - Hall
PI	proportional Integral
RF	Radio Frequency
SI	Système international
VCO	Voltage Controlled Oscillator

Contents

1 Introduction

Optical fibers are extremely useful waveguide for transferring laser light from one place to another allowing immense flexibility and convenience. Although remarkable advances in fabrication technology has made low dispersion and low attenuation fibers available, still remaining environmentally induced phase noise is critical for many high precision frequency based applications such as laser stabilisation and dissemination of optical clock standards.

Out of all measurable physical quantities, time and frequency can be measured with highest precision. Consequently, many precision measurements in science invariably require highly accurate and stable time or frequency reference. Today, atomic clocks set the standard of time providing time reference with uncertainty of 10^{-16} [1]. Optical clocks will provide substantially more precision (already demonstrated to have accuracy at 10^{-18} level [2] and has the potential to be better). The improved precision will be instrumental for innovations such as in advanced GPS and space-based navigation system, in relativistic geodesy and for new tests of fundamental constants variation. However, for distribution of optical frequency standards, frequency transfer through phase noise compensated fibers and laser stabilisation are most important prerequisites.

Apart from the perspective of the development of the optical clocks, fiber phase noise cancellation and laser stabilisation are also very crucial to quantum computation research. This thesis work has been carried out in the Quantum Information group at Atomic Physics Division of Lund University. To perform quantum computation experiments, the group requires ultra high stability laser system and is looking into ways of improving stabilisation using rare earth ion doped crystals. The idea is to create a spectral hole to induce slow light effect in the crystal cavity and then lock the laser to a resonance peak of the cavity for frequency stabilisation. Several parts of the system are connected using fiber links and these fibers are needed to be stabilised first. The aim of the thesis is to plan and design a setup for slow light crystal cavity locking, investigate how different parts can be constructed and finally carry out fiber stabilisation experiment.

1.1 Background

1.1.1 Fiber Phase Noise

In today's world, optical fibers are most widely used means of secure and efficient light transmission revolutionising the field of optics and communication. However, fibers are limited in their performance by various kinds of attenuation, dispersion and phase noises.

- Attenuation happens due to absorption and scattering effects in the medium and it limits the transmitted optical power.

- Dispersion is the temporal spread in the optical pulse and primary sources of dispersion are modal dispersion, material dispersion, polarization dispersion etc.

- The phase noise is introduced in the fiber by various environmental perturbations, temperature and pressure fluctuations, mechanical stretches and strains in the fiber etc.

Although a polarization maintaining single mode fiber can provide very low attenuation and dispersion, the remaining phase noise can often be not neglected for ultra high resolution applications and it is then necessary to compensate for the phase noise. The laser linewidth in a 25m long optical fiber cable has been measured to be broadened by 300 Hz [7]. Acoustic pressure variations can also add up to the phase noise leading to a broadening to 1kHz level [12].

An effective way to compensate the phase noise induced in the fiber is to retro-reflect some light through the fiber, then to detect the phase noise using heterodyne measurement and an error signal is generated from the phase noise which is sent to a regulator controlling a frequency modulator (such as Acousto-Optic Modulator) to modulate the laser beam and cancel the phase noise at the sender's end. Figure 1 shows the schematic diagram of this fiber noise cancellation method. The technique has been shown effective in canceling phase noise up to kHz level [7].

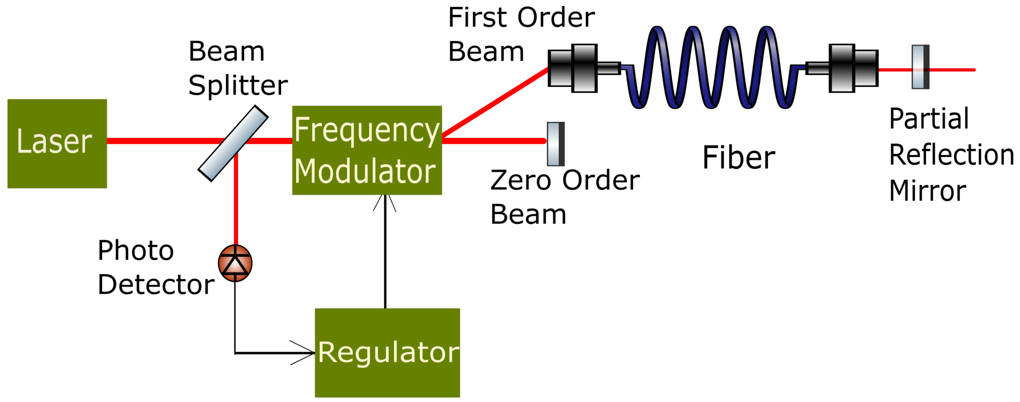

Figure 1: Fiber Noise Cancellation Schematic

1.1.2 Optical Clocks

At present, in SI unit system, the definition of second is based on atomic transition between two hyperfine levels of Caesium atom, which is in microwave regime [3]. Moving the reference transition frequency from microwave to the optical regime is the basis of optical clocks. Recent key advances in femtosecond frequency comb as frequency synthesizers, trapping of neutral atoms and single ions, laser frequency stabilisation - all have revolutionised the development of optical clocks.

Since the demonstration of frequency combs based on mode-locked femtosecond lasers, it has become possible to count the cycles of high optical frequency which is necessary for optical clockwork. Since then many different atomic systems have been investigated to be used as frequency reference for optical clocks such as single trapped $^{199}Hg^{+}$ ion as early as in 2001 [4] showing frequency instability of $7 \cdot 10^{-15}$ down to 10^{-17} in single trapped ion based clocks [5] and 10^{-18} in trapped neutral atoms based optical lattice clocks [2].

For standardisation of optical clocks, it is necessary to disseminate the frequency standards and remote comparison of the clocks. This means that stable and accurate frequency transfer over long distances is necessary. The conventional way of disseminating stable frequencies is via satellites. With this method transfer with a fractional uncertainty of 10^{-15} level can be achieved [6]. Although this stability is sufficient for microwave clocks, it is insufficient for the exploitation of the full potential of optical clocks. Hence, the frequency distribution through fiber links has been investigated, resulting recently in the frequency transfer over a distance of 1840 km in Germany[8] with a transfer instability of $4 \cdot 10^{-19}$. However, if the fiber noise cancellation is turned off, the phase noise induced in the fiber severely limits the performance (limits instability at 10^{-13} level[8]). This demonstrates that active phase noise cancellation for stabilising the fiber link is an essential requirement.

1.1.3 Frequency Stabilisation of a Laser

Laser frequency stabilisation is done by measuring the laser frequency in some way and feeding back this measurement to the laser control to cancel the frequency fluctuation. Frequency measurement can be done by sending the laser light to a reference Fabry-Perot cavity and then looking at the reflection or transmission. Optical cavities have evenly spaced transmission lines or resonance peaks (the spacing is called Free Spectral Range) as shown in figure 2(a) and 2(b). The laser can be locked to one of these resonance peaks to be stabilised. However, one problem is that both the transmission and the reflection have even symmetry around the resonance and when it drifts out of lock, it is not possible to tell which side of resonance it is.

An elegant and effective technique, Pound-Drever-Hall (PDH) locking, finds a way around to this problem. Figure 2(c) shows the basic setup for PDH locking. Frequency modulation is done using an Electro-Optic Modulator (EOM). Reflected light from the cavity is picked up by a photodetector, which is then sent to a mixer or phase detector. The mixer compares the signal with oscillator driving the EOM and generates an error signal (figure 2d) which is the indicative of the derivative of the reflected intensity. This signal is then fed back to a regulator which locks the laser to the cavity resonance peak.

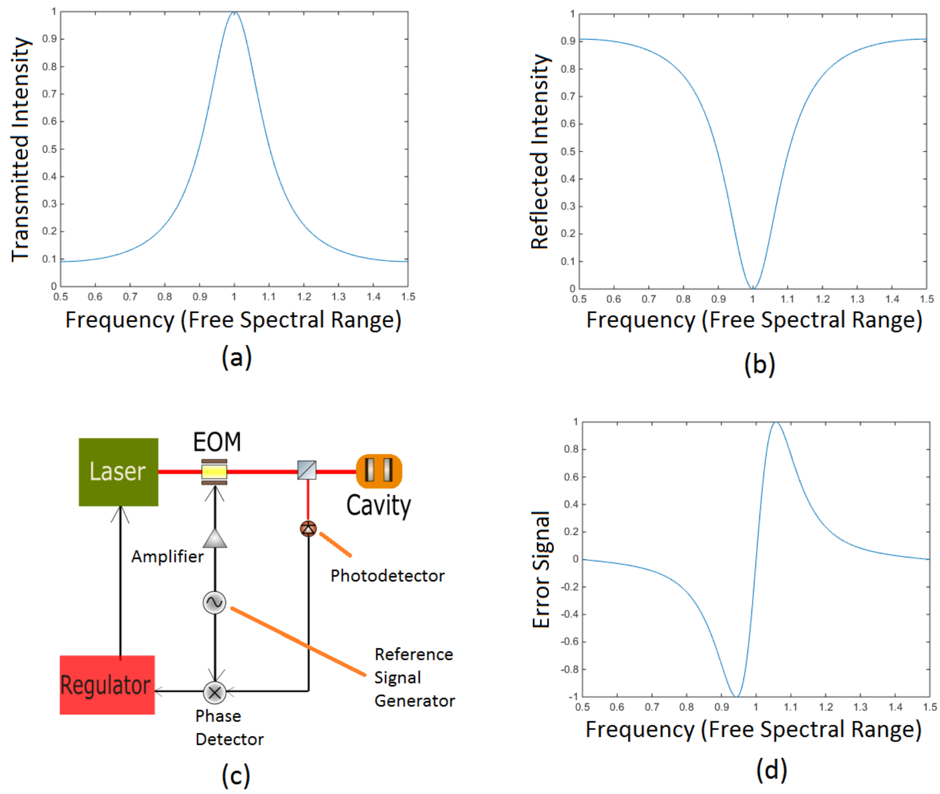

Figure 2: Laser Frequency Stabilisation (a) Transmitted Intensity in a Fabry - Perot Cavity (b) Reflected Intensity (c) PDH Locking Basic Setup (d) The error signal in PDH locking

1.1.4 Slow Light Crystal Cavity

Frequency stabilisation by locking the laser to a cavity is limited by the stability of the cavity itself. The cavity stability can be improved by choosing a longer cavity length but mechanical noise associated with it makes this quite impractical. One solution can be to use slow light effect which will allow increasing the effective cavity length without increasing the physical length of the cavity.

Slow light effect can be induced by a process known as spectral hole burning in a rare earth ion doped crystal. Due to doping, mechanical strain is introduced in the crystal which inhomogeneously broadens the absorption profile of the doping ions inside the crystal (figure 3a). If the laser is tuned to an arbitrarily chosen

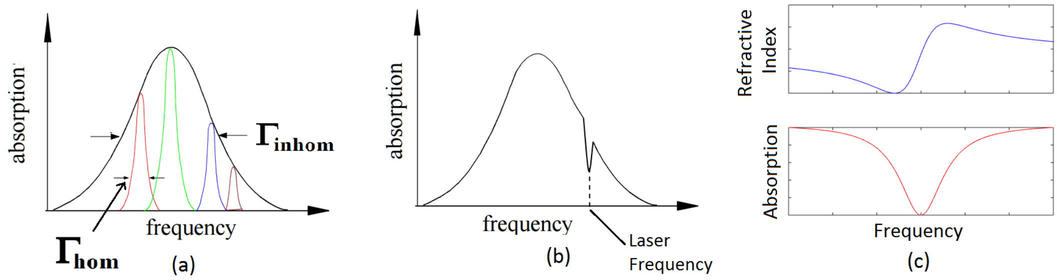

Figure 3: Spectral Hole Burning (a) Absorption profile for inhomogeneously broadened medium (b) A spectral hole is burnt at the laser frequency (c) Refractive index profile corresponding to a hole in the absortion profile

frequency within this inhomogeneously broadened profile, the ions having resonance in that frequency range will be excited to higher energy states and from there they can relax to a non-resonant state reducing absorption significantly. This creates a dip or "hole" in the absorption profile (figure 3b). A hole in the absorption profile corresponds to a steep gradient of refractive index as shown in figure 3(c). The group velocity of a light pulse depends on the slope of refractive index. As a result, the sharp gradient in the refractive index inside the hole will reduce the group velocity and hence induce slow light effect.

1.1.5 Feedback Control

When the desired output of a system is known, an optimum way to control the system output is to add a feedback loop. Figure 4 shows the general structure of a negative feedback system. “Plant” refers to the main system process. Input signal is the reference or the desired output for the system and the difference between the input and the output of the system is the error signal of the system. The error signal represents how much adjustment is needed to reach the desired response. “Controller” is the device which compensates the system and controls the operation of the feedback loop.

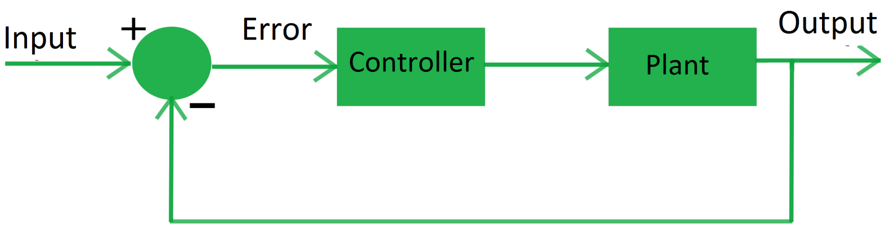

Figure 4: Negative Feedback Loop Diagram

Proportional-Integral (PI) controller is the most commonly used controller[11]. The input/output relationship of an ideal PI controller is following [14]:

$$u(t) = K_p e(t) + K_i \int_0^t e(t)dt = K_p \left(e(t) + \frac{1}{T_i} \int_0^t e(t)dt \right) \quad (1)$$

Here, $e(t)$ is the error signal of the system, $u(t)$ is the output of the controller, the control parameters are proportional gain K_p, Integral gain K_i and Integral Time constant T_i ($K_i = K_p/T_i$). From equation 1, the transfer function for the PI controller in the Laplace domain can be obtained:

$$G(s) = K_p + \frac{K_i}{s} = K_p + \frac{K_p}{sT_i} \quad (2)$$

Here, in the equation 2, s is a complex frequency variable in Laplace domain.

Lets consider proportional-only controller first. In this case, the control signal is controller gain multiplied by error signal. As the system approaches the desired response, the error signal gets smaller and smaller, which in turn decreases the control signal over time and error signal never becomes zero resulting in steady state error. By increasing the controller gain, the steady-state error can be reduced. However, if the gain is high enough, the system response becomes oscillatory. The controller acts like a restoring force against the direction of the error which can be thought of analogous to mass-spring system. So, the system output starts to oscillate.

By adding the integral part to the proportional controller, both the steady state error and oscillation problem can be eliminated. The integral term sums the error over time to compensate for the steady state error. It can be thought of automatic adjustment of offset with the proportional controller part. The integral gain K_i or time constant T_i controls how fast the system approaches the desired value. However, if the integral gain is set too high, the system response becomes oscillatory as explained before.

2 Method

2.1 Setup Schematics

2.1.1 Fiber Noise Cancellation Setup

The primary assumption for the working principle of the fiber noise cancellation method is that the optical fiber path has a negligible degree of non-linearity and non-reciprocity. This means that two optical signals going in opposite direction in an optical fiber will propagate independently and will have same phase noises independent of direction. Therefore, an optical signal if retransmitted back to the original source, will have twice the noise generated by the optical fiber path. Although the fluctuations in the phase noise are random, on average over time the total phase noise will be two times the noise induced in the fiber path. If the phase of the source optical light is pre-modulated with the negative of the phase noise generated by the path, then the output signal at the fiber end will be noise free compared to the source signal.

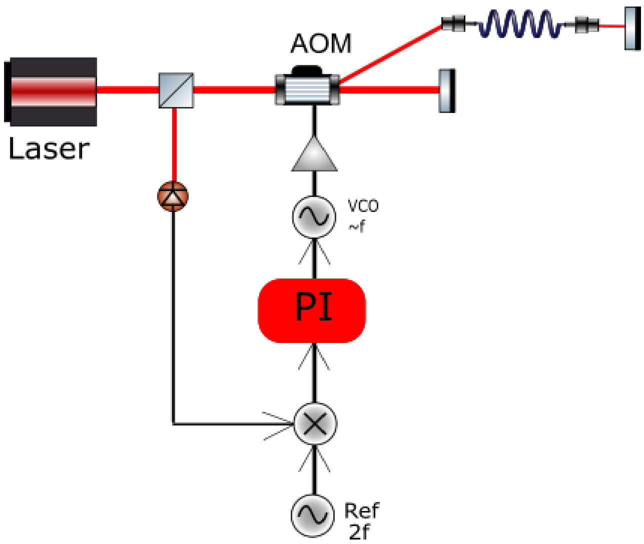

Figure 5: Fiber Noise Cancellation System

Figure 5 shows the block diagram of the fiber noise cancellation system. It is a feedback control system where an Acousto-Optic Modulator (AOM) is used as a frequency shifter. The AOM is driven by a Voltage Controlled Oscillator (VCO) which is driven by a Proportional-Integral Controller (PI). The source laser light propagates through the AOM and divides into two signals, the zero order beam and the first order diffracted beam. The first order beam is shifted by $f_{VCO} = f_{set} + \Delta f$ where f_{set} is the frequency set in the VCO and Δf is the modulation frequency proportional to the control signal output of the PI controller (V_{PI}).

The shifted first order beam is coupled into the optical fiber where it picks up phase noise after propagating the fiber. The phase noise broadens the linewidth of the laser light by Δf_n. The light is then partially reflected back from the far end of the fiber. Therefore, it picks up twice the phase noise and twice the broadening ($2\ \Delta f_n$) of the linewidth of the laser. Then, it is passed through the AOM again which shifts its frequency once more adding twice the frequency shift. The zero order beam is also reflected back and passed through the AOM again where it coincides with the first order diffraction signal. Using a beam splitter, the signal is directed to a photo detector which detects the beating frequency $2(f_{VCO} + \Delta f_n) = 2(f_{set} + \Delta f + \Delta f_n)$.

The electrical signal from the photo detector is fed into the mixer/phase detector where it is compared with a reference signal $f_{ref} = 2f_{set}$. The output from the phase detector contains the phase noise information and is the error signal for the system. The error signal is then fed into the PI controller. The output of the PI controller is the control signal for the VCO driving AOM. PI controller gain can be set by tuning such that the frequency modulation by the VCO, Δf compensates for the broadening Δf_n due to induced phase noise. Thus after locking, the output signal from the fiber is just frequency shifted by f_{set} but stabilised and without any phase noise.

2.1.2 Slow Light Crystal Cavity Locking Setup

Figure 6 shows the setup design for slow light crystal cavity locking. Rare earth ion doped crystals (such as Praseodymium (Pr^{3+}) doped in Yttrium Orthosilicate Y_2SiO_5) are usually chosen for slow light cavities since rare earth ions have large inhomogeneous broadening and long lifetime in hyperfine levels which result in better and longer persisting hole burning effects and larger slow light effects. To prevent thermal phonon excitations, the crystal is mounted inside a cryostat where it is kept at cryogenic temperatures. The laser system in the Quantum Information research lab is a dye laser pumped by $Nd{:}YVO_4$ laser. The dye laser is first pre-stabilized by locking to a reference cavity and the aim is to lock to the slow light crystal cavity for better and improved stabilisation. By comparing the stabilisation achieved by locking to the slow light cavity with the stabilisation obtained from locking to the reference cavity, the effects of slow light on laser stabilisation can be determined.

Two optical fibers are required: one connects the laser to the reference cavity and the other connects the laser to the optical table where the crystal is mounted inside the cryostat. Both of the fibers need to be stabilised and the same kind fiber locking system as described in previous section is employed. In both parts, beam sampler is used to partially reflect back light through the fiber. An AOM driven by an Arbitrary Waveform Generator (AWG520) does laser tuning to create the spectral hole burning. Once the burning is done, by switching the connection, the same AOM is used for frequency modulation in the PDH locking process. An oscillator drives an EOM through a high voltage amplifier. The EOM modulates the laser beam and the reflected light from the cavity is picked up by a photodetector. Signal output from the photodetector and the oscillator is sent to a phase detector which generates the error signal for the locking. This error signal is sent to a PI controller. The PI controller generates the control signal for the voltage control oscillator driving the AOM and closes the loop.

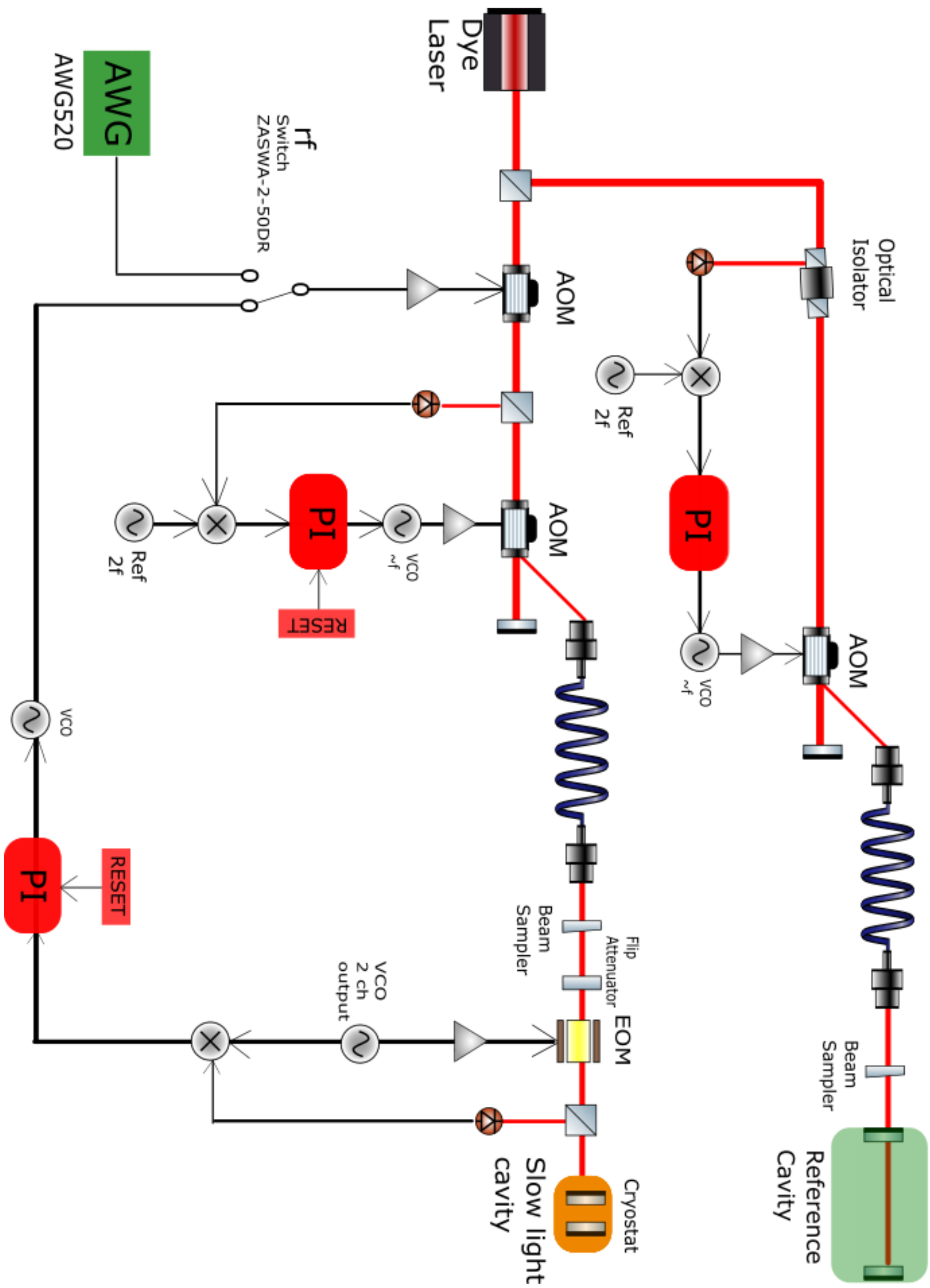

Figure 6: Slow Light Crystal Cavity Locking

The optical isolator performs two functions at the same time. It does not permit the beam come back to the laser cavity and also at the same time, it works as a beam splitter required for fiber locking setup. Back reflection from the reference cavity can form a cavity with the back reflection from the fiber. This can be avoided by having angled cleaving of the fiber instead of straight cleaving.

PI controllers work by integrating the error signal over time. Since the errors integrated in them during the hole burning are not relevant for locking purpose, the PI controllers need to be reset once the hole burning is done. Therefore, availability of PI controllers with reset function was investigated. The servo controller LB1005 has “integrator hold” function which can stop the integrating function during the hole burning though this function does not reset the integrator to zero.

After discussion with the research group, another alternative method was suggested. The fiber connected to the cryostat can be stabilised with another laser (He-Ne laser) and then the stabilisation can remain on without the need to reset the PI controllers. However, the He-Ne laser has to be stable enough that it has a coherence length fairly more than twice of the fiber length. Such a laser system was not found. Additionally, to combine this laser beam with the main dye laser beam, dichroic mirror is required in place of beam splitter and beam sampler which complicates the system. Due to these constraints, this approach of adding another He-Ne laser was discarded.

2.2 Selection of Suitable Components

2.2.1 Signal Generators

Signal generators are essential components of the fiber noise cancellation system and searching for suitable generators was the initial step for building the setup. Signal generators are required primarily for two purposes: 1. To be used as a Voltage Controlled Oscillator (VCO) and 2. To be used as reference oscillator for the phase detectors.

One RF signal will drive the AOM which has bandwidth in the region of 50 - 100 MHz and the other will be used for the reference signal and will have twice that frequency. Hence, the primary criteria for selecting the oscillator is that they should have output of sinusoidal radio waves with center frequency in the region of 50 - 200 MHz with very low phase noise. The other necessary requirement is that the oscillator should have external frequency modulation capability. For fiber noise cancellation system, the minimum modulation bandwidth requirement is 20 KHz. However, the signal generators are planned to be used for further applications in future projects (such as laser locking to slow light crystal cavity) where 1 MHz frequency modulation bandwidth will be required. Keeping that in mind, several solutions were investigated and table 1 shows the short-listed selection with relevant properties for comparison:

Company & Model	Frequency Range	FM Bandwidth	SSB Phase Noise
R & S SMJ100A	100 KHz to 3 GHz	10 MHz	-130 dBc
R & S SMV03	9 KHz to 3.3 GHz	1 MHz	-128 dBc
R & S SML01	9 KHz to 1.1 GHz	1 MHz	-128 dBc
R & S SMIQ03B	300 KHz to 3.3 GHz	2 MHz	-116 dBc

Table 1: Selection of Signal Generators (R & S Stands for Rohde & Schwarz)

Signal generators are quite costly. Because of comparatively high price and lack of availability, the models SMJ100A and SMV03 were rejected. Finally, it was decided that we would buy three signal generators: two units of model SML01 and one unit of SMIQ03B.

The signal generators that were already existed in the lab were : Novatech 425A DDS and one VCO based on AD9912 DDS, constructed by previous master student Anders Ronneholm as part of his master project [10]. The Novatech 425A DDS has output range up to 350 MHz, but does not have frequency modulation capability.

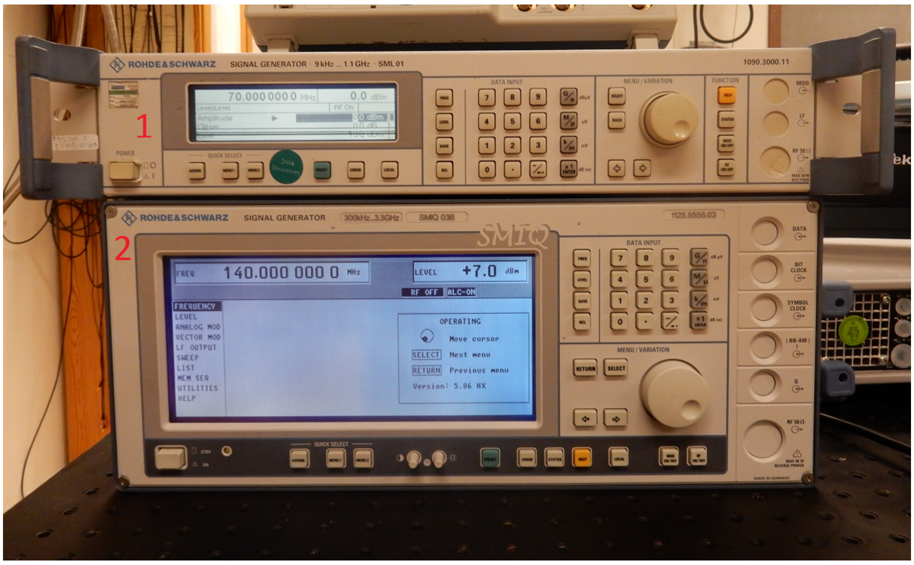

Figure 7: Signal Generators. Marked as 1 is the model R&S SML01 and marked as 2 is the model R&S SMIQ03B

The other VCO has frequency modulation range upto 250 KHz. These two signal generators were initially used to test the AOM setup but due to their limitations, we eventually switched to the Rohde & Schwartz signal generators.

2.2.2 Servo Controller

The PI controller used in the set-up is the LB1005 High-Speed Servo Controller from the United States based company New Focus. The PI controller has large bandwidth (10 MHz) particularly suited for the regulation required to stabilize intensity and frequency of various laser systems. Figure 8 shows the front panel of the instrument used in the experiment.

Figure 8: LB1005 High Speed Servo Controller

The controller takes two BNC inputs A and -B (marked 1 in the figure 8) and error signal is generated from their voltage difference. Single ended operation (as in the case of this experiment) can be done by simply leaving one input channel open. The error signal can be monitored using the output channel Error Monitor (marked 5). The Input Offset knob can provide stable offset voltage to the error signal but was disabled using a rear panel switch as it was not necessary for the purposes of the experiment. The BNC Output channel (marked 4) provides the control signal from the controller, has an impedance of 50 Ohm and a drive current of $\pm 20mA$. The filter section (marked as 6) has three knobs for three tuning parameters: Gain Knob, P-I Corner knob and LF Gain Limit.

The PI controller has three work modes which can be selected by a switch (marked as 8). In the "Lock Off" mode, the integrator is turned off and no control signal is added to the output. The "LFGL" mode is the low frequency gain mode where the DC gain of the integrator is limited as determined by the LF Gain Limit switch in the filter sections. The final mode is the "Lock on" mode where the full integrator is enabled. Depending on the situation and requirement, “LFGL” mode can be helpful to find the lock and acquire intermediate lock particularly where it becomes necessary to limit DC gain.

There is also a led light indicator which shows the operating status of the controller. The led color is normally red but it changes to green if the system acquires lock. The controller consider itself to be in lock position if the both of the following two conditions are met:

- Error Signal voltage is within $\pm 0.33V$
- Output Signal voltage is not within 10% of either the positive or negative output voltage limits.

2.2.3 Phase Detector

The RPD-2 phase detector from MiniCircuits was used. It has bandwidth from 5 Mhz to 150 MHz. It has three input/output channels: RF, IF and LO. RF channel takes the rf signal input and LO takes the reference signal input. IF generates the phase detector output signal which is the difference frequency/phase between the RF and LO signals.

2.2.4 Photodetector

The photodetector used is custom built by Thorlabs based on the Photodetector PDA10BS-AC. The photodetector has bandwidth 1-150 MHz. It has a Silicon based P-i-N photodiode which has detection wavelength range is 350 nm to 1060 nm and responsivity of 0.375 A/W at the wavelength 632 nm. The photocurrent generated by the photodiode is then amplified by an Op-Amp with a transimpedance gain of $1.65 \cdot 10^4$ V/A which is the RF output of the photodetector.

2.2.5 Acousto-Optic Modulator

The AOM used was 1205C-2 AOM from Isomet Corp. The center frequency of the AOM is 80 MHz and it works with good diffraction efficiency in the range of 60 - 100 MHz (specified to be 85% at 80 MHz). With 2 mm active aperture size, it provides good both single and double pass frequency shifting capability.

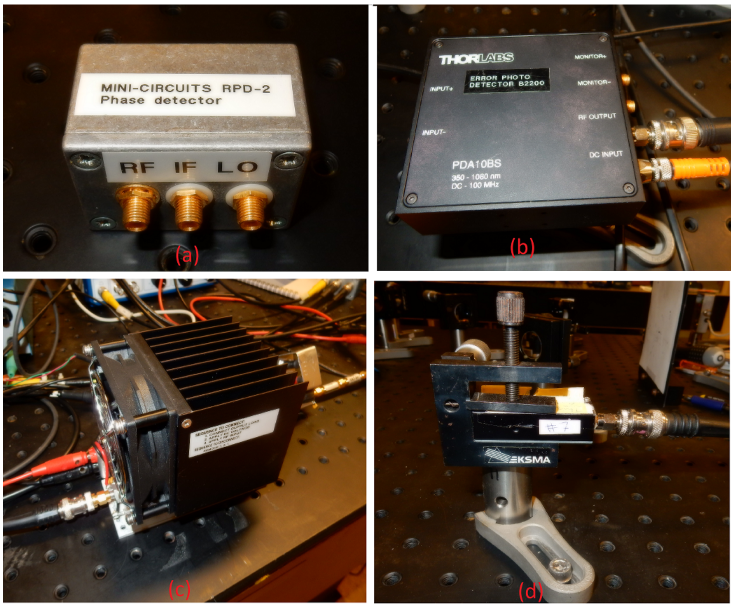

Figure 9: Electronic Components: (a) Phase Detector (b) Photodetector (c) RF Amplifier (d) Acousto-optic Modulator

2.2.6 Optics

- Mirrors - Throlabs BB-1 E02 Broadband Dielectric mirrors
- Lenses - Thorlabs 25.4 mm diameter, Spherical lenses with focal length of 500 mm, 200 mm.
- Beam Splitter - Thorlabs BSW10 50:50 UV Fused Silica Broadband Plate Beamsplitter
- Aperture

The other electronics components that were used in the set-up are following:

- RF Amplifier - ZHL-03-5WF
- Attenuators - Model HAT-3, HAT-2 etc.
- High Power Attenuators - BW-S10W20 - 10 dB attenuation, maximum working power 20W
- Low Pass Filter

These components were from MiniCircuits.

2.3 Building the Locking System

The laser used in the setup is a stabilized Helium-Neon laser from Spectra -Physics (Model 117A). The laser output wavelength is 632.8 nm and maximum output optical power is 4.5 mW with a beam diameter of 0.5 mm. The unit has a user selectable key to work between two modes: frequency stabilized and intensity stabilized. For the purposes of the setup, frequency stabilized mode was selected and in this mode, the laser is stabilized within a few megahertz level.

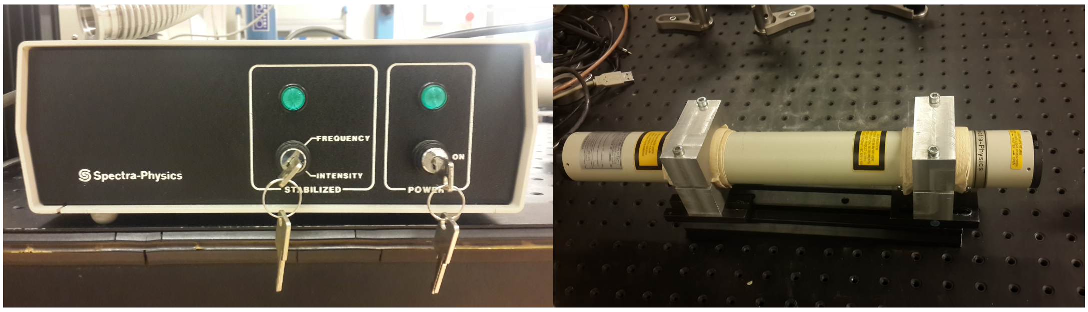

Figure 10: The He-Ne Laser system (a) Laser Driver Control (b) The cavity of the laser

2.3.1 Setting Up the AOM

An Acousto-Optic Modulator (AOM) is a frequency shifter device based on acousto-optic effect and can be controlled by a radio frequency (RF) signal. The main component of an AOM is a transparent crystal through which the light propagates. The applied RF signal induces an acoustic wave in the crystal medium which then creates a periodic refractive index in the medium similar to diffraction grating. A light beam travelling through the medium now will experience diffraction and the angle of diffraction θ can be determined by Bragg's law:

$$m\lambda = 2d \sin \theta \tag{3}$$

Here, λ is the wavelength of the travelling light wave, d is the distance between acoustic grating lines and m is the order of the diffracted beams (m = 0, 1, -1, 2, -2 etc). Since the acoustic grating is generated by sound wave propagating through the medium, the diffracted light beams will be Doppler shifted in frequency. The frequency shift of the diffracted beams are given by:

$$\Delta f = m \cdot f_{RF} \tag{4}$$

Here f_{RF} is the frequecny of applied RF signal. From equation 4, the frequency shift for zero order beam is zero and for first order beam is f_{RF}. Figure 11 shows the basic principle of diffraction in the AOM.

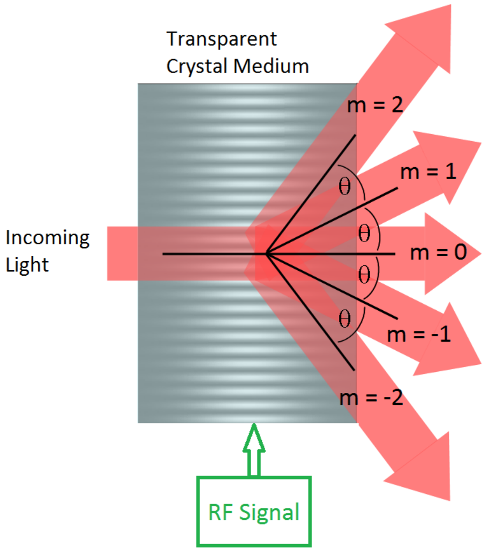

Figure 11: Basic Principle of an Acousto-Optic Modulator

Figure 12 shows the schematic diagram for AOM driver setup. For maximum diffraction efficiency, the drive power is needed to be around 1W or 30 dBm. The signal generators does not provide rf signal at that power level. Hence, an rf amplifier (ZHL-03-5WF) was used which can provide a gain around 35 dB. A drive power more than 1W or 30 dBm can be harmful for the AOM. Therefore, attenuators were used also in conjunction with the amplifier to generate the appropriate power level. Before applying the drive signal to the AOM, the signal power level was tested using oscilloscope. High power attenuators (BW-S10W20) were used to protect the oscilloscope from damage.

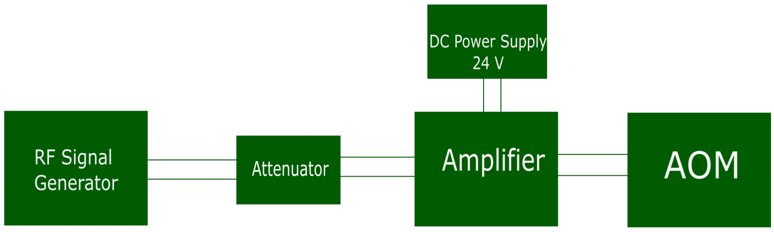

Figure 12: Schematic diagram for AOM driver setup

When applying the RF signal to the AOM, the connections to the amplifier needs to be made in correct order to protect the amplifier. First the output load (AOM) needs to be connected, then the DC supply voltage and finally the RF signal is connected. While disconnecting the amplifier, the sequence must be reversed.

For the RF signal, three signal generators were tested sequentially. First, the Novatech 425A DDS was used. The rf signal output from the DDS can be controlled by PC using serial communication terminal software (such as HyperTerminal) and sending command through the terminal. The other signal generator which was custom built based on AD9912 DDS also requires connection with a PC to control the output signal. Because of their limitation in frequency modulation, we eventually switched to the R&S SML01 signal generator. It also provides more flexibility in use as the device has built-in knobs for all the output control options and does not require a PC connection. The AOM was operated with 70 MHz Rf signal.

The diffraction efficiency of the AOM depends on proper beam alignment, Bragg angle adjustment and RF power drive. The laser beam was controlled using a mirror to properly align the beam height and position with the AOM aperture. Bragg angle can be adjusted using the knobs attached to the holder of the AOM. After optimising the Bragg angle and beam alignment, the RF power drive was increased gradually to find the maximum diffraction efficiency.

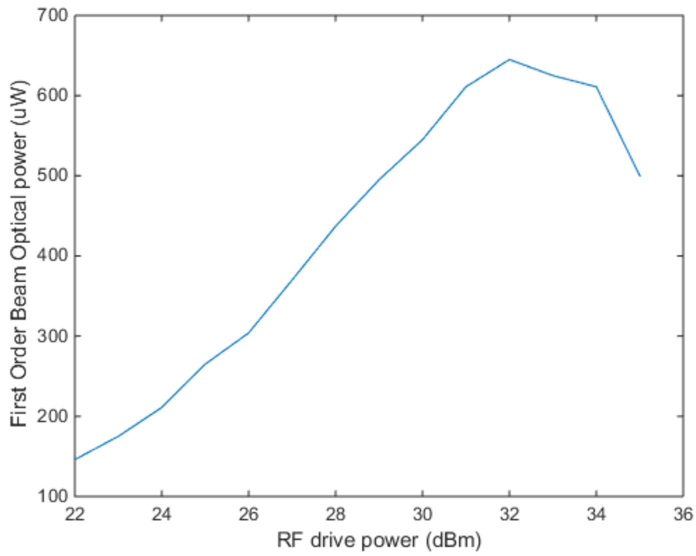

Figure 13: First order diffracted beam power at different RF drive power

The figure 13 shows the optical power of the first order diffracted beam at different RF drive power. The optical power was measured using an optical power meter. The RF signal was connected with an oscilloscope with a channel impedance of 50 Ω where the RMS (Root Mean Square) voltage of the signal was determined which was then converted to dBm unit. The maximum first order beam optical power was measured at 32 dBm RF drive power. The diffracted beam power increases linearly with RF drive power until it reaches the maximum point and after that the power decreases.

$$\text{Transmission} = \frac{\text{Zero Order Beam Power(AOM off)}}{\text{Input Laser Beam Power}} = \frac{870\mu W}{1.12mW} = 77.67\%$$

$$\text{Diffraction Efficiency} = \frac{\text{First Order Beam Power}}{\text{Zero Order Beam Power(AOM off)}} = \frac{645\mu W}{870\mu W} = 74.13\%$$

The Total Efficiency = Transmission * Diffraction Efficiency = 57.57%

(a)

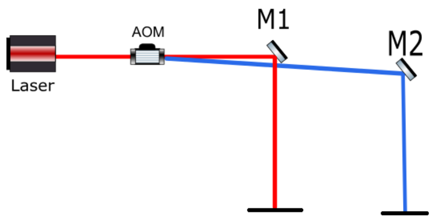

(b)

Figure 14: (a) Clear Edge Mirror Mount (b) Beam Separation Schematics. Red color is the zero order beam and the blue color is the first order shifted beam. The mirror M1 has the clear edge mount

The separation angle between the zero order beam and the first order beam is on the order of milliradians (calculated to be 12 mrad from the specifications). Thus the two beams are very close and needs to be separated. One way to separate the two beams is to mount a mirror in a clear edge type mount as shown in the figure 14 (a). The edge of the mirror is exposed which allows the first order beam to pass through but reflects the zero order beam from its edge.

2.3.2 Testing the Photodetector

Figure 15 (a) shows the setup schematics for testing the photodetector B2200. The zero order beam and the first order beam are superimposed using a beam splitter and then directed to the photodetector sensitive area through a lens. Both the beams interfere with each other and the beating signal is detected in the photodetector.

Detection efficiency depends on the spatial alignment of the wavefronts of the two overlapped beams. If the beams are misaligned, detection will be much less. One way to keep the beams sufficiently aligned is to make sure that both the beams are fairly overlapped in a range of ∼2 m.

Another factor for better detection efficiency is to match the radius of curvature of both the wavefronts. Laser beams propagating in different optical path can have different beam divergences. Figure 15 (b) shows the radius of curvature of wavefronts of two beams with different divergences. If the curvature difference is too great, detection will be much less. Differing curvature can be matched using

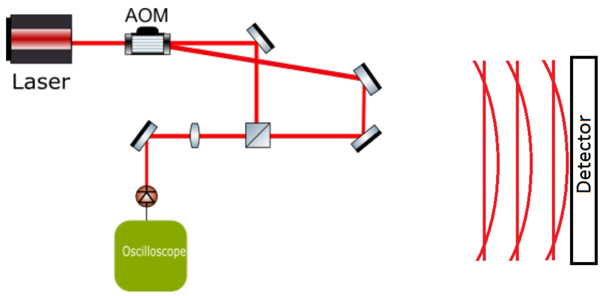

(a) (b)

Figure 15: (a) Schematics for beat note generation (b) Wavefronts of two beams with different radius of curvature at the detector

optical lenses.

Next the double pass feedback configuration (as figure 5) was setup without coupling the fiber with the first order beam to test the locking electronics. Both the first order and the zero order beams were reflected back through the AOM and their beating signal was detected. Then the beating signal was mixed with reference $2f_{ref}$ signal generated by another signal generator (R&S SMIQ03B) in a phase detector and output from this was the error signal. The error signal was then connected to the PI controller which controls the feedback action.

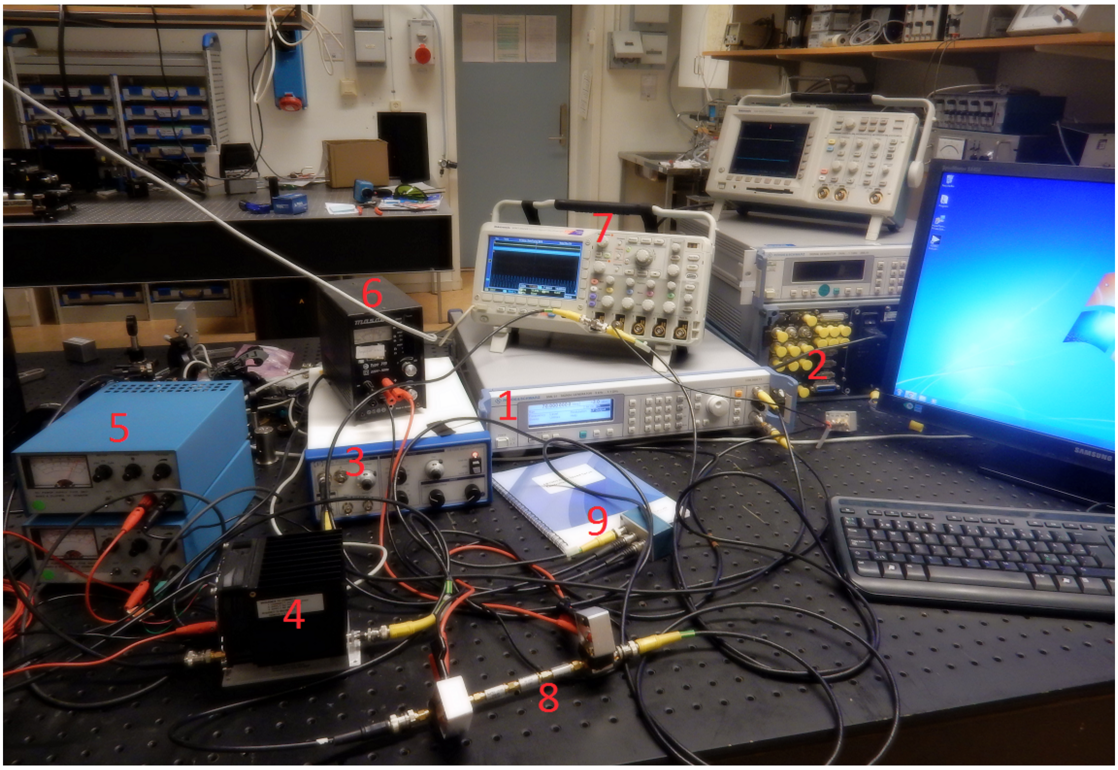

Figure 16: Locking electronics arrangement. (1) Signal generator working as VCO (2) The reference signal generator (3) The PI controller (4) RF amplifier driving the AOM (5) & (6) DC power supply (7) Tektronix Oscilloscope (8) Small signal rf amplifiers and attenuators to amplify beating signal sent to the phase detector (9) The phase detector.

2.3.3 Locking with PI controller

First step of operation of the PI controller was to check and set two safety settings: fuse settings and Output Voltage Limit settings. The controller has two different fuse ratings for different AC main voltages. It was factory pre-configured for American AC main standard (110 V), hence fuse setting was required to change for use in 220 V supply voltage. As per instruction manual provided with the controller, appropriate fuse was installed on the power entry module located on the rear panel. The second safety setting was to set the Output Voltage Limit. In the rear panel, there are two potentiometers which sets the positive and negative voltage limit of the output signal. The controller output is the modulation signal for the VCO. SML01 R&S signal generator is being used as the VCO and it takes modulation signal for frequency modulation in the range of $\pm 1V$. The output voltage of the controller was set to be limited within this range.

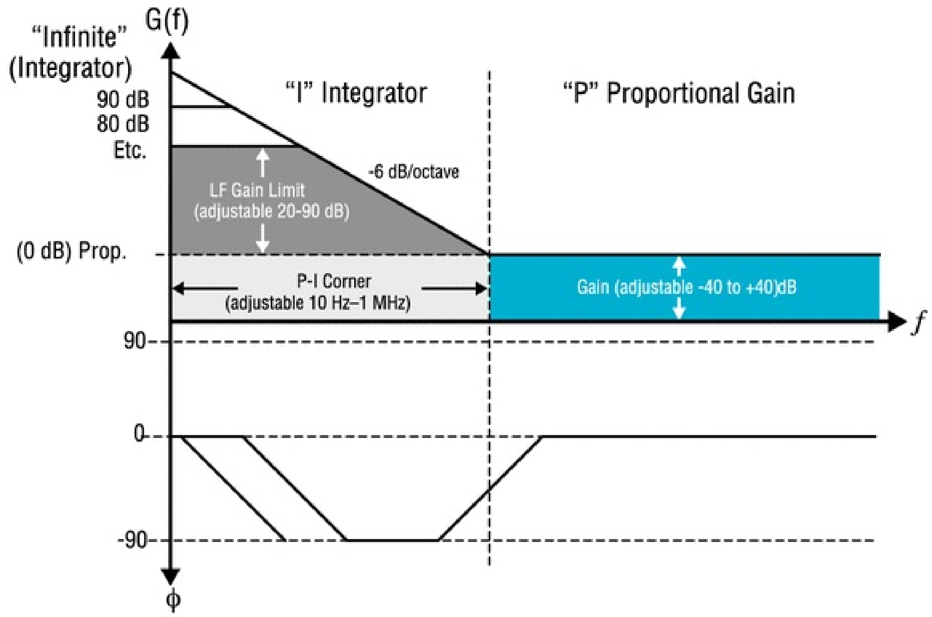

Figure 17: PI controller filter gain frequency response [13]

The analog signal processing in the servo controller is done in three stages: Input stage, Filter stage and Output stage. Filtering is the most important part and controls the behavior of the system response. Figure 17 shows the frequency response of the gain of the filter.

Three user controlled parameters sets the operation of the filter: Gain (K), the P-I Corner Frequency (f_{PI}) and optional LF Gain Limit. Gain sets the overall proportional gain of the feedback loop. The PI corner frequency is the 3 dB break frequency for the filter and its the tuning parameter for the integral action part. Exceeding this point, proportional gain dominates over integral gain.

Mathematical function in the Laplace domain for the output of the filter in "Lock-on" mode is given by:[13]

$$V_{control}(s) = V_{error}(s)K\left(1 + \frac{2\pi f_{PI}}{s}\right) \tag{5}$$

So, the gain of the filter is:

$$G(s) = K\left(1 + \frac{2\pi f_{PI}}{s}\right) = K + \frac{2\pi f_{PI}}{s}K \tag{6}$$

Comparing equation 6 with equation 2 (gain for a general PI controller), we get:

$$\text{Proportional Gain, } K_p = K$$

$$\text{Integral Time Constant, } T_i = \frac{1}{2\pi f_{PI}}$$

2.3.4 Fiber Coupling and fiber locking

After the beam separation, next step was to couple the first order beam with an optical fiber and from the far end, reflect back the beam through the fiber. Figure 18 shows the fiber coupling setup. The optical fiber used is 3m long. Both end of the fiber is connected to fiber collimators, C1 and C2 in the figure. The first order beam is controlled by two mirrors M1 and M2 and sent to the C1 collimator. An aperture is placed between these two mirrors to block diffracted beams except the first order beam. A focus adjustable lens is attached to the C1 collimator by mounting in a cage system where the separation between the lens and the collimator is adjustable. Thus the two mirrors M1 and M2 and the separation between the lens and the collimator provides five degrees of freedom to align the beam with the fiber. After proper alignment, the light beam was coming out at the other end of the fiber through the C2 collimator. A beam splitter with 70% reflectivity was used to reflect back the light through the fiber.

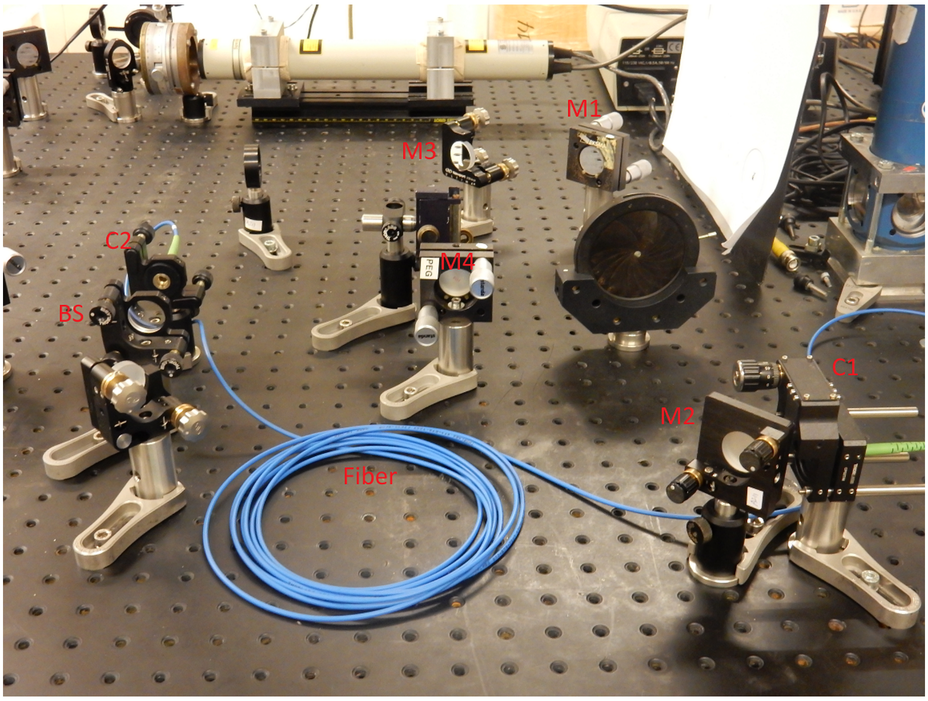

Figure 18: Fiber Coupling Setup

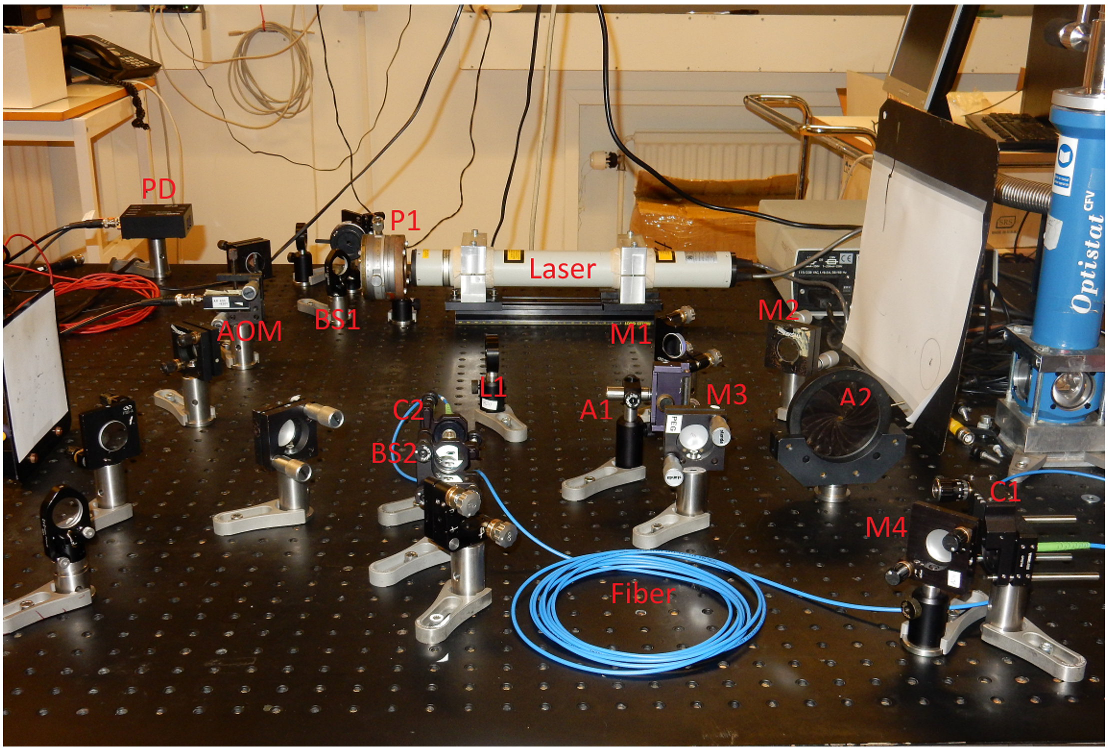

Figure 19: Complete Optical Setup. The zero order beam is controlled and reflected back using mirrors M1 and M3. The first order beam is coupled with the fiber using mirrors M2 and M4 and collimator C1. Beamsplitter BS2 relfects the light back through the fiber. The beam size of the reflected beams were larger than the aperture of AOM. The lens L1 is placed to collimate the reflected beams. Both the reflected beams are overlapped and sent to the photodetector PD using the 50:50 beamsplitter BS1. Polarisation of the laser beam is controlled using the polariser P1.

3 Results & Discussions

3.1 Testing the Fiber Locking

The fiber locking using the PI controller can be checked by observing the two input signals of the phase detector simultaneously while triggering on one of them. From the figure 5, the two input signals of the phase detector are the beating signal between the reflected zero and first order beam, and the reference signal. If the locking is working, these two signals will be phase locked to each other and if one signal is connected as a trigger to oscilloscope, the other will appear stable in phase. Figure 20 shows the signals observed when the reference signal was connected to the oscilloscope as trigger.

When the locking is off (figure 20a), it can be observed that the phase of the beating signal is fluctuating a lot compared to the phase of the reference signal. This fluctuation is due to the phase noise induced by the optical fiber and since locking is off, the phase noise is not being compensated. When the locking is on, the locking electronics compensates for the phase noise and as can be observed from figure 20b, the beating signal appears to be stable in phase although there are still some remaining phase noise. It is also evident that both the signals have same phase which means phase angles for the waveforms of both the signals remain same with time. Hence, it can be concluded that both the signals are phase locked and fiber locking is working.

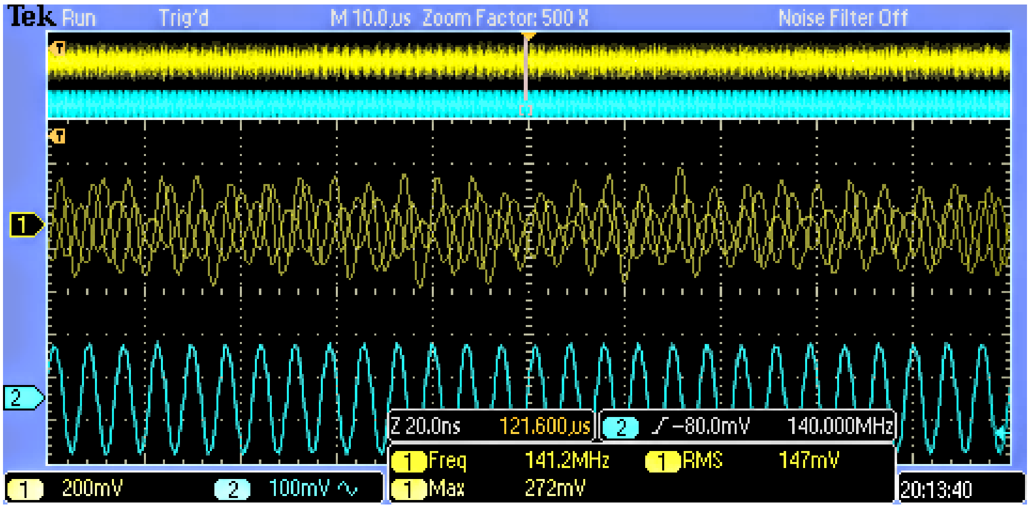

(a) When locking is off

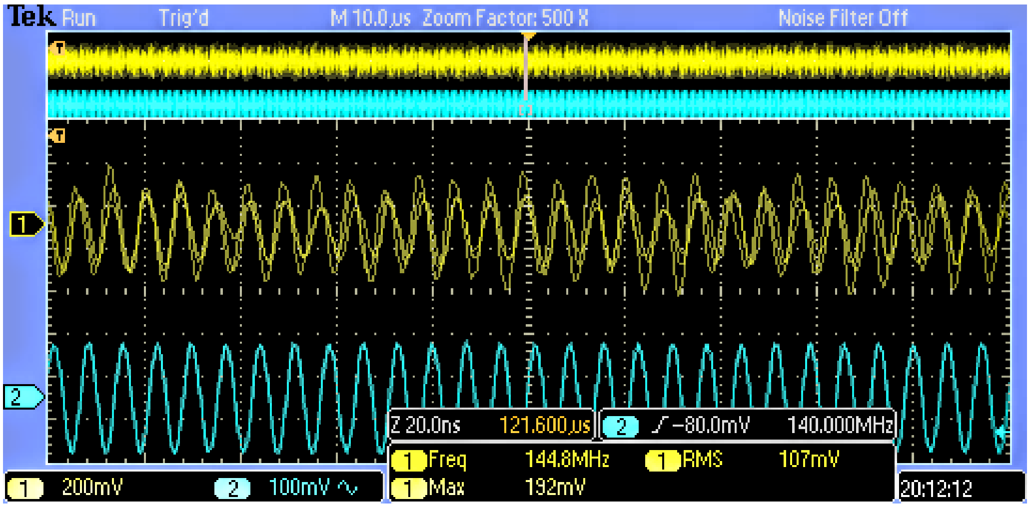

(b) when locking is on

Figure 20: Phase Locking: Channel 1 (yellow) is the beating signal and channel 2 (blue) is the reference signal.

For further analysis, the error signal of the system is observed, both when the locking is off and when the locking is on (figure 21 and figure 22 respectively). The error signal is the output of the phase detector and represents the phase difference between the two input signals of the phase detector. If the two signals are phase locked to each other, the fluctuation in the error signal will decrease. Comparing both of the figures, it can be observed that, when the locking is on, the fluctuation in the error signal is reduced as expected. The small scale fluctuation in the error signal means there are still some remaining phase noise.

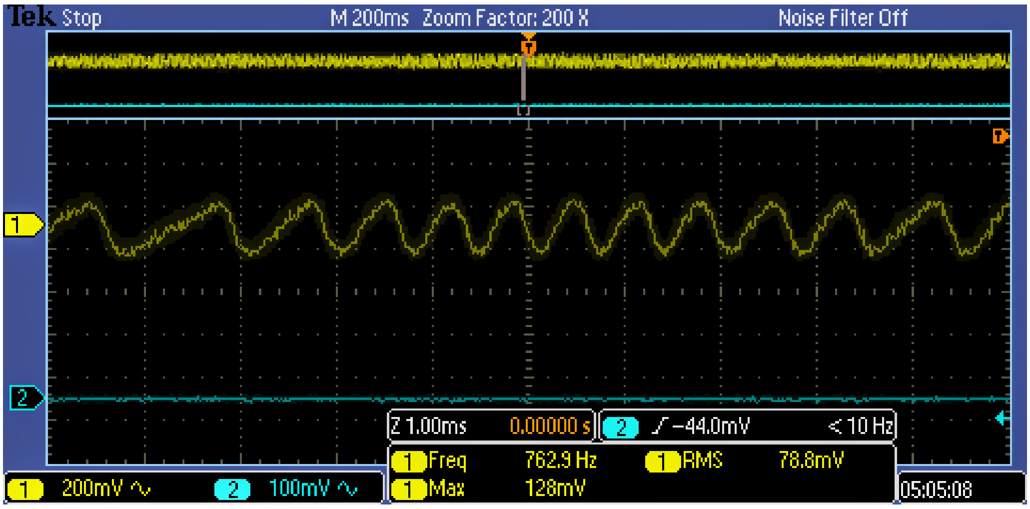

Figure 21: Error Signal: When locking is off

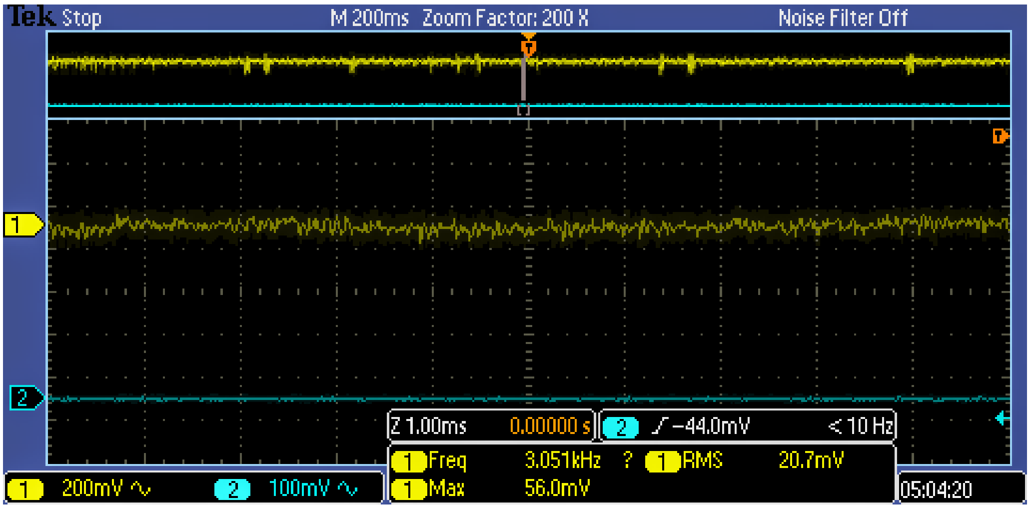

Figure 22: Error Signal: When locking is on

3.2 Conclusion and Outlook

The aim of the thesis was to design and build a fiber phase noise cancellation system for a laser locking experiment. Although fiber locking was achieved, because of lack of time, measurement was not done to estimate how much phase noise was cancelled and how much stability was gained by the system. The light beam coming out of the fiber can be superimposed with the original laser beam and the beating signal generated can be detected and analysed in a Spectrum Analyzer to determine the gained stability. Moreover, this spectrum analysis can also be useful for further fine tuning experimentation to improve locking or stability.

The next step for the project is to continue to the rest of the laser locking experiment according to the setup plan shown in figure 6. However, there are several issues to be resolved before carrying out that experiment. In this thesis project, fiber locking experiment was done using a He-Ne laser. Fiber locking with the dye laser stabilised by a reference cavity needs to be investigated. Moreover, the issue of resetting the integrator of the PI controller is yet to be resolved.

In conclusion, research on laser frequency stabilisation and fiber stabilisation has advanced tremendously in recent decades with the developments of optical clocks and quantum information science. The application of slow light effects by spectral hole burning might unravel new potentials to meet the demand of ultra high precision in these fields.

References

[1] Parker T. E. *Long-term comparison of caesium fountain primary frequency standards.* Metrologia, 47 (2010).

[2] Bloom B. J., Nicholson T. L., Williams J. R., Campbell S. L., Bishof M., Zhang X., Zhang W., Bromley S. L. and Ye J. *An optical lattice clock with accuracy and stability at the* 10^{-18} *level.* Nature, 506, 71–75 (2014).

[3] `http://physics.nist.gov/cuu/Units/second.html`

[4] Diddams S. A., Udem Th., Bergquist J. C., Curtis E. A., Drullinger R. E., Hollberg L., Itano W. M., Lee W. D., Oates C. W., Vogel K. R. and Wineland D. J. *An Optical clock based on a single trapped* $^{199}Hg^{+}$ *ion.* Science, Vol. 293 (2001).

[5] Rosenband T., Hume D. B., Schmidt P. O., Chou C. W., Brusch A., Lorini L., Oskay W. H., Drullinger R. E., Fortier T. M., Stalnaker J. E., Diddams S. A., Swann W. C., Newbury N. R., Itano W. M., Wineland D. J. and Bergquist J. C. *Frequency ratio of* Al^{+} *and* Hg^{+} *single-ion optical clocks, Metrology at the 17th decimal place.* Science, Vol. 319 (2008)

[6] Bauch A., Achkar J., Bize S., Calonico D., Dach R., Hlavac R., Lorini L., Parker T., Petit G. and Piester D. *Comparison between frequency standards in Europe and the USA at the* 10^{-15} *uncertainty level.* Metrologia, 43 (2005).

[7] Long-Sheng Ma, Peter Jungner, Jung Ye and John L.Hall. *Optics Letters Vol.19, No. 21. Delivering the same optical frequency at two places: accurate cancellation of phase noise introduced by an optical fiber or other time-varying path.* Optics Letters, Vol. 19, No. 21 (1994).

[8] Droste S., Ozimek F., Udem Th., Predehl K., Hänsch T. W., Schnatz H., Grosche G. and Holzwarth R. *Optical-Frequency Transfer over a Single-Span 1840 km Fiber Link.* Phys. Rev. Lett. 111, 110801 (2013).

[9] Black E.D. *An introduction to Pound–Drever–Hall laser frequency stabilization.* Am. J. Phys. 69, 79 (2001).

[10] Ronnholm, A. *Fiber noize cancellation.* Master Thesis. Division of Atomic Physics, Lund University (2012).

[11] Astrom K.J. and Hagglund T. *The future of PID control.* Control Engineering Practice, Vol. 9, No. 11. (2001).

[12] Pang Y., Hamilton J. J. and Richard J. *Frequency noise induced by fiber perturbations in a fiber-linked stabilized laser.* Appl Opt. 31(36):7532-4. (1992).

[13] LB1005 Servo Controller Manual. `http://assets.newport.com/webDocuments-EN/images/LB1005OperatingManualP2102297revA.PDF`

[14] Astrom K.J. and Murray R. M. *Feedback Systems: An Introduction for Scientists and Engineers.* Princeton University Press, 2nd Edition (2009).